



## Curcumin-Loaded Solid Lipid Nanoparticles from *Curcuma longa* Attenuate Inflammatory Cytokine Cascades in a Rat Model of Acute Peritonitis

Oliva Azalia Putri<sup>1\*</sup>, Dedi Sucipto<sup>2</sup>

<sup>1</sup>Department of Thoracic Surgery, CMHC Research Center, Palembang, Indonesia

<sup>2</sup>Department of Internal Medicine, Phlox Institute, Palembang, Indonesia

### ARTICLE INFO

#### Keywords:

Acute peritonitis  
Curcumin  
*Curcuma longa*  
Herbal nanomedicine  
Solid lipid nanoparticles

#### \*Corresponding author:

Oliva Azalia Putri

#### E-mail address:

[oliva.azalia@cattleyacenter.id](mailto:oliva.azalia@cattleyacenter.id)

All authors have reviewed and approved the final version of the manuscript.

<https://doi.org/10.37275/ehi.v6i1.137>

### ABSTRACT

Acute peritonitis remains a life-threatening intra-abdominal inflammatory condition with significant morbidity and mortality, particularly in resource-limited settings across Southeast Asia. Curcumin, the principal polyphenol of *Curcuma longa* L. (Zingiberaceae), has potent anti-inflammatory and antioxidant properties, but its clinical use is limited by poor oral bioavailability, rapid hepatic metabolism, and low aqueous solubility. This study evaluated the anti-inflammatory and antioxidant efficacy of curcumin-loaded solid lipid nanoparticles (Cur-SLNs) in a cecal ligation and puncture (CLP)-induced acute peritonitis rat model. Thirty male Wistar rats were randomized into five groups (n=6): sham, CLP+vehicle, CLP+free curcumin (100 mg/kg), CLP+Cur-SLN low dose (50 mg/kg), and CLP+Cur-SLN high dose (100 mg/kg). Cur-SLNs prepared by hot homogenization-ultrasonication had a mean particle size of 152.4±8.7 nm, polydispersity index 0.218±0.03, zeta potential -28.6±2.1 mV, and entrapment efficiency 87.3±3.2%. At 24 hours, Cur-SLN high dose significantly reduced TNF- $\alpha$  (89.6±18.3 versus 287.5±45.2 pg/mL, p<0.001), IL-6 (102.4±22.7 versus 312.4±52.8 pg/mL, p<0.001), and IL-1 $\beta$  (78.5±16.8 versus 245.6±41.3 pg/mL, p<0.001) compared with CLP-vehicle, with large effect sizes (Cohen's d 4.50–5.72), alongside attenuated oxidative stress, reduced bacterial burden, and preserved peritoneal histology. Cur-SLNs from *Curcuma longa* represent a promising herbal nanomedicine strategy for attenuating inflammatory cascades in acute peritonitis.

### 1. Introduction

Acute peritonitis is a severe intra-abdominal inflammatory condition characterized by peritoneal membrane inflammation resulting from bacterial contamination, visceral organ perforation, or post-operative complications, representing one of the most critical surgical emergencies worldwide. Intra-abdominal infections are the second most common cause of sepsis in critically ill patients, and reported mortality for peritonitis and related intra-abdominal infections ranges widely, from approximately 5% to 50% depending on disease severity, comorbidity burden, and the degree of organ dysfunction.<sup>1</sup> In Southeast Asian countries, including Indonesia, the

burden of peritonitis is disproportionately elevated due to delayed presentation, limited access to advanced surgical facilities, and the rising prevalence of antimicrobial-resistant organisms, with case fatality rates that may exceed 30% when complicated by sepsis and multi-organ dysfunction.<sup>1</sup>

The pathophysiology of acute peritonitis involves a complex interplay of innate immune activation, inflammatory cytokine cascades, and oxidative stress amplification. Upon peritoneal contamination, resident macrophages and recruited neutrophils initiate a robust inflammatory response through pattern recognition receptors, particularly Toll-like receptor 4 (TLR4) and nucleotide-binding oligomerization domain (NOD) receptors.<sup>2,3</sup> This

activation triggers downstream signaling through the MyD88 adaptor, culminating in nuclear factor kappa-light-chain-enhancer of activated B cells (NF- $\kappa$ B) nuclear translocation and transcription of pro-inflammatory mediators including tumor necrosis factor- $\alpha$  (TNF- $\alpha$ ), interleukin-6 (IL-6), interleukin-1 $\beta$  (IL-1 $\beta$ ), cyclooxygenase-2 (COX-2), and inducible nitric oxide synthase (iNOS).<sup>2</sup> Concurrently, the overwhelming inflammatory response generates excessive reactive oxygen species (ROS), depleting endogenous antioxidant defenses such as superoxide dismutase (SOD), catalase, and glutathione peroxidase, perpetuating a vicious cycle of oxidative tissue injury and inflammatory amplification.<sup>3</sup>

Conventional management relies on source-control surgery combined with broad-spectrum antibiotic therapy. However, the escalating crisis of antimicrobial resistance, particularly among Gram-negative pathogens such as extended-spectrum beta-lactamase (ESBL)-producing Enterobacterales and carbapenem-resistant *Acinetobacter baumannii*, has severely compromised standard antibiotic regimens.<sup>4</sup> Furthermore, antibiotic therapy alone inadequately addresses the dysregulated inflammatory cascade and oxidative stress burden that contribute to tissue destruction and organ failure, catalyzing a paradigm shift toward integrative strategies that combine conventional antimicrobials with complementary anti-inflammatory and antioxidant agents derived from natural sources.<sup>5</sup>

Curcumin (diferuloylmethane, C<sub>21</sub>H<sub>20</sub>O<sub>6</sub>, molecular weight 368.38 g/mol) is the principal curcuminoid polyphenol isolated from the rhizome of *Curcuma longa* L. (turmeric, Zingiberaceae), a perennial herb widely cultivated across tropical regions of Indonesia, India, and Southeast Asia.<sup>5,6</sup> In traditional Indonesian jamu medicine, turmeric rhizome preparations — known locally as “jamu kunyit” — have been used for centuries as anti-inflammatory, wound-healing, and antimicrobial remedies for abdominal complaints and gastrointestinal disorders.<sup>6</sup> This extensive ethnobotanical heritage provides a robust cultural and empirical foundation for the modern scientific

investigation of curcumin's therapeutic potential in inflammatory conditions.<sup>5</sup>

The rhizome of *Curcuma longa* contains approximately 2–5% curcuminoids by dry weight, comprising curcumin (60–80%), demethoxycurcumin (15–27%), and bisdemethoxycurcumin (3–6%), along with volatile oils (3–7%) such as ar-turmerone and zingiberene.<sup>5,6</sup> Structurally, curcumin possesses a symmetrical bis- $\alpha,\beta$ -unsaturated  $\beta$ -diketone backbone whose  $\alpha,\beta$ -unsaturated carbonyl groups serve as Michael acceptor sites, enabling covalent modification of nucleophilic cysteine thiol residues on target proteins.<sup>7</sup> Curcumin's pleiotropic anti-inflammatory mechanisms include direct inhibition of NF- $\kappa$ B activation through suppression of I $\kappa$ B kinase (IKK) phosphorylation, downregulation of COX-2 and 5-lipoxygenase expression, and attenuation of mitogen-activated protein kinase (MAPK) signaling.<sup>3,7</sup> Additionally, curcumin activates the nuclear factor erythroid 2-related factor 2 (Nrf2)/heme oxygenase-1 (HO-1) antioxidant defense pathway by modifying Keap1 cysteine residues (Cys151, Cys273, Cys288), disrupting the Keap1–Nrf2 complex and enabling Nrf2 nuclear translocation and binding to antioxidant response elements (ARE).<sup>8</sup>

Despite these properties, the clinical translation of curcumin has been constrained by poor oral bioavailability (less than 1% in humans), attributable to low aqueous solubility, extensive first-pass hepatic metabolism, rapid intestinal metabolism, and alkaline-pH degradation, necessitating innovative delivery strategies.<sup>9</sup>

Solid lipid nanoparticles (SLNs), first developed in the early 1990s, have emerged as a promising colloidal carrier system for lipophilic bioactives. SLNs comprise a solid lipid matrix (e.g., glyceryl monostearate) stabilized by surfactants, forming spherical particles of 50–1000 nm.<sup>10</sup> Advantages include enhanced bioavailability through lymphatic uptake, sustained release, improved stability, biocompatibility, and scalability.<sup>10,11</sup> Curcumin-loaded SLNs (Cur-SLNs) substantially enhance the apparent bioavailability, stability, and sustained release of curcumin relative to the free compound.<sup>11,13</sup> Hamdalla et al.<sup>12</sup> reported that

curcumin nanoparticles markedly downregulated TNF- $\alpha$ , IL-6, and IL-1 $\beta$  together with NF- $\kappa$ B and iNOS in an experimental inflammation model, while Khatri et al.<sup>10</sup> demonstrated that solid lipid nanoparticle encapsulation improved curcumin solubility, entrapment efficiency, and controlled release. Montanino et al.<sup>9</sup> further showed in a clinical study that a standardized water-soluble turmeric formulation produced greater systemic anti-inflammatory activity than conventional fat-soluble curcumin, underscoring the bioavailability gains achievable through formulation.

To date, no study has specifically evaluated Cur-SLNs in attenuating inflammatory cascades in acute peritonitis, despite the strong pathophysiological rationale for targeting NF- $\kappa$ B-mediated inflammation and oxidative stress. The aim of this study was to evaluate the anti-inflammatory and antioxidant efficacy of curcumin-loaded solid lipid nanoparticles prepared from *Curcuma longa* L. rhizome extract in a cecal ligation and puncture-induced acute peritonitis model in Wistar rats, with focus on pro-inflammatory cytokine attenuation, oxidative stress modulation, bacterial burden reduction, and peritoneal tissue preservation.

## 2. Methods

### **Study design and ethical approval**

This randomized controlled experimental study was conducted at the Eureka Research Laboratory, Indonesia, between January and June 2024. The protocol was reviewed and approved by the CMHC Ethics Committee (Approval No. CMHC/EC/2024/0147) in accordance with the Declaration of Helsinki and the National Guidelines for Health Research Ethics of the Republic of Indonesia. All animal procedures adhered to the NIH Guidelines for the Care and Use of Laboratory Animals (NIH Publication No. 85-23, revised 2011) and the ARRIVE guidelines version 2.0. Treatment allocation used computer-generated randomization by an independent statistician. The surgeon performing CLP was blinded to treatment assignments, and all outcome assessments were conducted by blinded investigators. With power 0.80,

$\alpha=0.05$ , and an anticipated large effect size, the minimum required sample size was  $n=5$  per group (G\*Power 3.1.9.7);  $n=6$  per group was used to allow for attrition.

### **Plant material, authentication, and curcumin extraction**

Fresh rhizomes of *Curcuma longa* L. (local cultivar “*Kunjit Palembang*”) were procured from a certified Good Agricultural Practices herbal farm in South Sumatra, Indonesia. Botanical authentication was performed by a taxonomist, and a voucher specimen (CL-2024-015) was deposited at the university herbarium; HPTLC fingerprinting confirmed identity against the reference *Curcuma longa* profile. Dried, milled rhizome (moisture <10%, 60-mesh) underwent maceration with 96% ethanol (1:10 w/v, 72 h), vacuum filtration, and rotary evaporation at 40 °C (crude yield 8.7% w/w). The extract was purified by silica-gel column chromatography and characterized by HPLC (Shimadzu LC-20AD; C18 column; UV 425 nm), confirming curcumin purity of 96.3% (retention time 8.42 min) matching the reference standard (Sigma-Aldrich C1386,  $\geq 98\%$ ). Total curcuminoid content comprised curcumin (78.2%), demethoxycurcumin (16.4%), and bisdemethoxycurcumin (5.4%).

### **Preparation and characterization of Cur-SLNs**

Cur-SLNs were prepared by hot homogenization-ultrasonication. The lipid phase (glyceryl monostearate 500 mg, soy lecithin 100 mg, purified curcumin 50 mg) was melted at 80 °C; the aqueous phase (Poloxamer 188 1% w/v, Tween 80 0.5% w/v) at the same temperature was added under high-speed homogenization (Ultra-Turrax T25, 12,000 rpm, 10 min) followed by probe ultrasonication (40% amplitude, 5 min, pulsed) on ice, then rapid cooling to 4 °C. Blank SLNs (vehicle) were prepared without curcumin. Particle size, polydispersity index (PDI), and zeta potential were measured by dynamic light scattering (Zetasizer Nano ZS90). Entrapment efficiency (EE) was determined by ultracentrifugation (100,000  $\times$  g, 30 min, 4 °C) with HPLC quantification of free curcumin, where  $EE (\%) = [(Total\ curcumin - Free\ curcumin) / Total\ curcumin] \times 100$ . The optimized formulation exhibited a mean particle size

of 152.4±8.7 nm, PDI 0.218±0.03, zeta potential -28.6±2.1 mV, and EE 87.3±3.2% (inter-batch coefficient of variation <6%); accelerated stability testing (25 °C/60% relative humidity, 3 months) showed <5% change in particle size and <3% curcumin loss.

### **Dose rationale, animals, and experimental groups**

Curcumin doses of 50 mg/kg (low) and 100 mg/kg (high) for intraperitoneal administration were selected by allometric scaling from traditional human dosing and prior preclinical studies; the human equivalent dose of 100 mg/kg in rats corresponds to approximately 16.1 mg/kg, within the safe and active clinical curcumin range (500–2000 mg/day).<sup>5,9</sup> Thirty male Wistar rats (*Rattus norvegicus*), aged 10–12 weeks and weighing 200–240 g, were housed under standard conditions (22±2 °C, 55±10% relative humidity, 12-hour light/dark) with free access to AIN-93M chow and purified water. After 7-day acclimatization, rats were randomized into five groups (n=6): Group 1 (Sham, laparotomy + vehicle); Group 2 (CLP+Vehicle); Group 3 (CLP+Free Curcumin, 100 mg/kg); Group 4 (CLP+Cur-SLN Low, 50 mg/kg); and Group 5 (CLP+Cur-SLN High, 100 mg/kg). Intraperitoneal treatments were given immediately after wound closure and again at 12 hours post-CLP.

### **Cecal ligation and puncture, sampling, and outcomes**

Acute peritonitis was induced by the standardized cecal ligation and puncture (CLP) technique by a single surgeon. Under ketamine (80 mg/kg)/xylazine (10 mg/kg) anesthesia, the cecum was ligated at 75% of its length and punctured twice with an 18-gauge needle; sham animals underwent cecal manipulation

only. At 24 hours, rats were euthanized by cardiac exsanguination per AVMA Guidelines (2020). Outcomes included serum TNF- $\alpha$ , IL-6, and IL-1 $\beta$  by ELISA (R&D Systems); serum malondialdehyde (MDA) by thiobarbituric acid reactive substances; serum SOD activity (Cayman Chemical); total white blood cell (WBC) count; peritoneal bacterial colony-forming units (CFU) by serial dilution (10<sup>-1</sup> to 10<sup>-6</sup>); and histopathological scoring of H&E-stained peritoneal tissue (0–4 scale) by two blinded pathologists (Cohen's kappa = 0.85).

### **Statistical analysis**

Data are expressed as mean±standard deviation (SD). Analyses used SPSS version 26.0. Normality (Shapiro-Wilk) and homogeneity of variances (Levene) were confirmed (all p>0.05). One-way analysis of variance (ANOVA) compared the five groups, with partial eta-squared ( $\eta_p^2$ ) as effect size, followed by Tukey's post-hoc test. Pairwise effect sizes were calculated as Cohen's d. A Bonferroni-corrected threshold of  $\alpha=0.006$  was applied; all primary comparisons remained significant. A two-tailed p<0.05 was considered significant.

## **3. Results and Discussion**

### **Animal characteristics and baseline parameters**

Baseline characteristics of the experimental animals are detailed in Table 1. There were no statistically significant differences among the five groups in body weight (F(4,25)=0.17, p=0.942,  $\eta_p^2=0.027$ ), age (F(4,25)=0.30, p=0.871,  $\eta_p^2=0.046$ ), or baseline WBC count (F(4,25)=0.11, p=0.956,  $\eta_p^2=0.017$ ), confirming successful randomization. As shown in Table 1, the mean body weight across all groups was 216.5±11.8 g, and all thirty animals survived the 24-hour experimental period.

Table 1. Baseline characteristics of the experimental animals (mean±SD, n=6 per group).

Parameter	Sham	CLP+Vehicle	CLP+Free Cur	Cur-SLN Low	Cur-SLN High
<b>Body weight (g)</b>	218.3±9.2	214.7±10.1	217.5±11.3	216.8±10.7	215.2±12.4
<b>Age (weeks)</b>	10.8±0.4	10.9±0.5	10.7±0.4	10.8±0.5	10.9±0.4
<b>Baseline WBC (10<sup>3</sup>/<math>\mu</math>L)</b>	9.1±1.5	9.3±1.4	9.0±1.3	9.2±1.6	9.1±1.4

Notes: WBC, white blood cell count; Cur, curcumin; SLN, solid lipid nanoparticles; SD, standard deviation.

These baseline findings support the internal validity of the randomization process and ensure that observed treatment effects are attributable to the interventions rather than pre-existing group disparities. Identical anesthetic protocols across all groups controlled for any confounding effect of ketamine–xylazine on inflammatory marker levels.

### Effects on pro-inflammatory cytokines

The effects of Cur-SLN treatment on serum pro-inflammatory cytokine levels at 24 hours post-CLP are summarized in Table 2 and illustrated in Figure 1. As shown in Figure 1, CLP-induced peritonitis produced dramatic elevation of all three cytokines compared with the sham group: TNF- $\alpha$  increased 6.8-fold (287.5 $\pm$ 45.2 versus 42.3 $\pm$ 8.7 pg/mL,  $p$ <0.001, Cohen's  $d$ =7.52), IL-6 increased 8.7-fold (312.4 $\pm$ 52.8 versus 35.8 $\pm$ 7.2 pg/mL,  $p$ <0.001,  $d$ =7.34), and IL-1 $\beta$  increased 8.6-fold (245.6 $\pm$ 41.3 versus 28.4 $\pm$ 6.5 pg/mL,  $p$ <0.001,  $d$ =7.35), validating the CLP model as an effective inducer of systemic inflammation

consistent with the cytokine-storm pathophysiology of polymicrobial sepsis.<sup>2</sup>

As detailed in Table 2 and Figure 1, Cur-SLN high dose (100 mg/kg) produced the most pronounced anti-inflammatory effect, reducing TNF- $\alpha$  by 68.8% (89.6 $\pm$ 18.3 pg/mL; mean difference -197.9 pg/mL, 95% CI -243.2 to -152.6;  $p$ <0.001,  $d$ =5.72), IL-6 by 67.2% (102.4 $\pm$ 22.7 pg/mL;  $p$ <0.001,  $d$ =5.17), and IL-1 $\beta$  by 68.0% (78.5 $\pm$ 16.8 pg/mL;  $p$ <0.001,  $d$ =5.30) versus CLP-vehicle. Cur-SLN low dose (50 mg/kg) also produced significant reductions (TNF- $\alpha$  50.4%, 142.7 $\pm$ 28.5 pg/mL; IL-6 47.1%, 165.3 $\pm$ 30.6 pg/mL; IL-1 $\beta$  45.9%, 132.8 $\pm$ 25.4 pg/mL; all  $p$ <0.001). Free curcumin at the equivalent 100 mg/kg dose achieved more modest reductions in TNF- $\alpha$  (41.4%), IL-6 (36.2%), and IL-1 $\beta$  (35.6%), with all comparisons between free curcumin and Cur-SLN high dose reaching significance ( $p$ <0.001 for TNF- $\alpha$  and IL-1 $\beta$ ;  $p$ =0.002 for IL-6), demonstrating the clear superiority of the nanoparticle formulation.

Table 2. Effects of Cur-SLN treatment on pro-inflammatory cytokines and oxidative stress markers (mean $\pm$ SD,  $n$ =6 per group).

Parameter	Sham	CLP+Vehicle	CLP+Free Cur	Cur-SLN Low	Cur-SLN High
TNF- $\alpha$ (pg/mL)	42.3 $\pm$ 8.7	287.5 $\pm$ 45.2	168.3 $\pm$ 32.1	142.7 $\pm$ 28.5	89.6 $\pm$ 18.3
IL-6 (pg/mL)	35.8 $\pm$ 7.2	312.4 $\pm$ 52.8	199.2 $\pm$ 38.5	165.3 $\pm$ 30.6	102.4 $\pm$ 22.7
IL-1 $\beta$ (pg/mL)	28.4 $\pm$ 6.5	245.6 $\pm$ 41.3	158.1 $\pm$ 29.7	132.8 $\pm$ 25.4	78.5 $\pm$ 16.8
MDA (nmol/mL)	1.8 $\pm$ 0.4	8.7 $\pm$ 1.6	5.2 $\pm$ 1.1	4.3 $\pm$ 0.9	2.8 $\pm$ 0.6
SOD (U/mL)	145.2 $\pm$ 18.3	62.4 $\pm$ 12.7	89.5 $\pm$ 15.8	105.3 $\pm$ 14.2	128.7 $\pm$ 16.5

Notes: TNF- $\alpha$ , tumor necrosis factor- $\alpha$ ; IL-6, interleukin-6; IL-1 $\beta$ , interleukin-1beta; MDA, malondialdehyde; SOD, superoxide dismutase; Cur, curcumin; SLN, solid lipid nanoparticles.

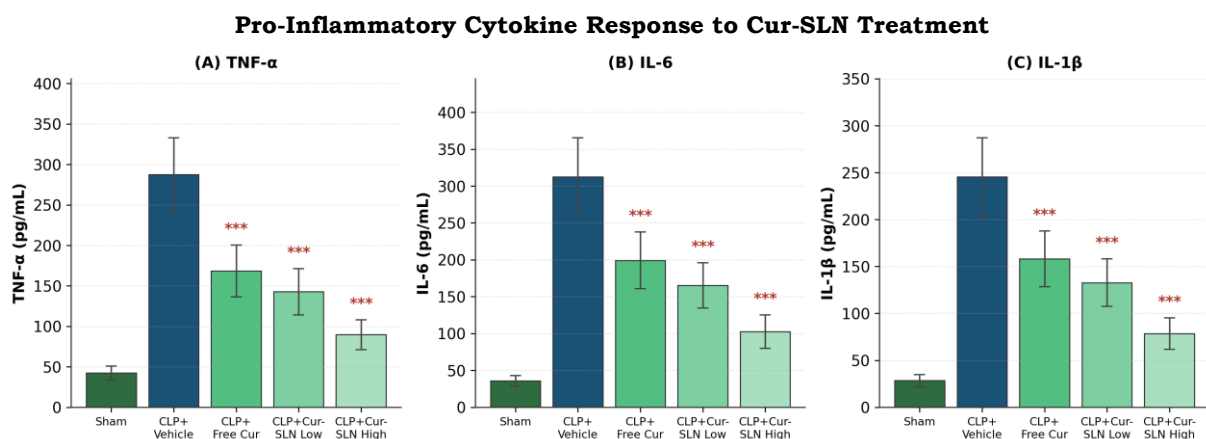


Figure 1. Serum pro-inflammatory cytokine levels at 24 hours post-CLP. (A) TNF- $\alpha$ , (B) IL-6, and (C) IL-1 $\beta$  across treatment groups, showing dose-dependent reduction with Cur-SLN treatment. Data are mean $\pm$ SD ( $n$ =6). \*\*\* $p$ <0.001 versus the CLP-vehicle group. Cur, curcumin; SLN, solid lipid nanoparticles.

The magnitude of cytokine suppression with Cur-SLN high dose (approximately 68%) is consistent with, and in several respects exceeds, that reported for nanoparticulate curcumin in comparable inflammatory models. Hamdalla et al.<sup>12</sup> demonstrated that curcumin nanoparticles significantly downregulated TNF- $\alpha$ , IL-6, and IL-1 $\beta$  alongside NF- $\kappa$ B and iNOS in an experimental arthritis model, while Javed et al.<sup>14</sup> observed marked reductions in IL-1 $\beta$ , IL-6, and TNF- $\alpha$  following intraperitoneal curcumin nanoparticle administration in a crystal-induced inflammatory model. The enhanced efficacy of Cur-SLNs may reflect pharmacokinetic advantages conferred by the solid lipid matrix: protection from degradation in the peritoneal microenvironment, sustained release, enhanced uptake by peritoneal macrophages, and improved intracellular delivery to NF- $\kappa$ B signaling compartments.

The anti-inflammatory mechanism of Cur-SLNs involves multi-target suppression of the NF- $\kappa$ B pathway. Through its  $\alpha,\beta$ -unsaturated carbonyl (Michael acceptor) moieties, curcumin directly inhibits IKK phosphorylation via covalent modification of the catalytic cysteine residue (Cys179) in IKK $\beta$ , preventing I $\kappa$ B $\alpha$  degradation and blocking NF- $\kappa$ B p65/p50 nuclear translocation, thereby suppressing transcription of TNF- $\alpha$ , IL-6, IL-1 $\beta$ , COX-2, and iNOS.<sup>7</sup> Curcumin additionally modulates upstream TLR4/MyD88 signaling, reducing the innate immune over-activation characteristic of polymicrobial peritonitis.<sup>3</sup> The dose-dependent response supports a concentration-dependent inhibition of NF- $\kappa$ B activation. The very large effect sizes observed in this controlled

preclinical setting (Cohen's  $d$  4.50–5.72) would likely translate to more moderate but still clinically meaningful effects in human disease.

In the context of Indonesian traditional medicine, these findings provide a mechanistic basis for the empirical use of *Curcuma longa* preparations in abdominal inflammatory conditions.<sup>5</sup> Nanoformulation amplifies curcumin's intrinsic anti-inflammatory potential to a degree relevant for acute inflammatory conditions, with implications for modernizing Indonesian traditional medicine within the evidence-based fitofarmaka framework established by BPOM (Badan Pengawas Obat dan Makanan).

### Effects on oxidative stress markers

Oxidative stress parameters are presented in Table 2 and illustrated in Figure 2. As shown in Figure 2, CLP-induced peritonitis caused a 4.8-fold increase in serum MDA (8.7 $\pm$ 1.6 versus 1.8 $\pm$ 0.4 nmol/mL,  $p$ <0.001,  $\eta_p^2$ =0.89) and a 57.0% decrease in SOD activity (62.4 $\pm$ 12.7 versus 145.2 $\pm$ 18.3 U/mL,  $p$ <0.001,  $\eta_p^2$ =0.91) compared with sham. Cur-SLN high dose significantly attenuated MDA elevation (2.8 $\pm$ 0.6 nmol/mL; 67.8% reduction;  $p$ <0.001,  $d$ =4.87) and preserved SOD activity (128.7 $\pm$ 16.5 U/mL; 106.3% increase versus CLP-vehicle;  $p$ <0.001,  $d$ =4.50). As detailed in Figure 2, Cur-SLN low dose also improved both markers (MDA 4.3 $\pm$ 0.9 nmol/mL, 50.6% reduction; SOD 105.3 $\pm$ 14.2 U/mL, 68.8% increase; both  $p$ <0.001), while free curcumin produced intermediate effects (MDA 5.2 $\pm$ 1.1 nmol/mL; SOD 89.5 $\pm$ 15.8 U/mL; both  $p$ <0.001 versus CLP-vehicle).

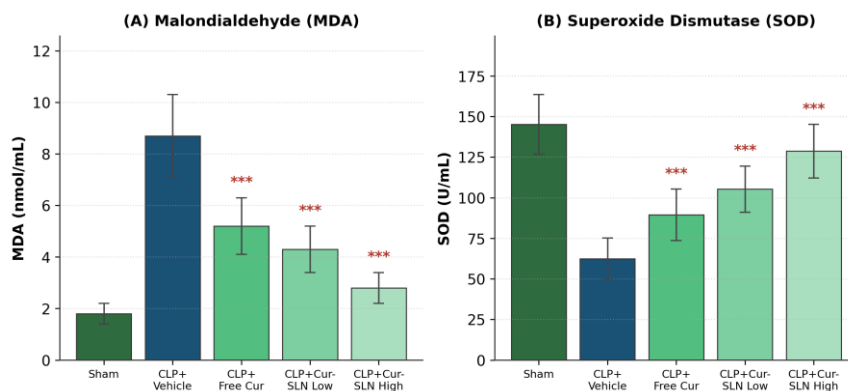


Figure 2. Oxidative stress markers at 24 hours post-CLP. (A) Malondialdehyde (MDA) and (B) superoxide dismutase (SOD) across treatment groups. Data are mean $\pm$ SD ( $n$ =6). \*\*\* $p$ <0.001 versus the CLP-vehicle group.

The superior antioxidant effect of Cur-SLNs is consistent with Chen et al.<sup>18</sup>, who showed that curcumin nanoparticle delivery enhanced free-radical scavenging while elevating SOD and reducing MDA in an oxidatively injured rat model. Curcumin acts through dual mechanisms: direct scavenging of ROS via hydrogen atom transfer from the phenolic hydroxyl groups of the feruloyl rings,<sup>5</sup> and indirect upregulation of endogenous antioxidant defenses via the Nrf2/Keap1 pathway, in which curcumin's electrophilic carbonyl groups undergo Michael addition with Keap1 cysteine residues (Cys151, Cys273, Cys288), releasing Nrf2 for nuclear translocation and ARE binding to upregulate SOD, catalase, glutathione peroxidase, and HO-1.<sup>8</sup> The preserved SOD activity in the Cur-SLN high dose group (88.6% of sham) suggests effective Nrf2 activation, corroborated by Tanase et al.<sup>8</sup>, who detailed curcumin-mediated disruption of the Keap1-Nrf2 complex with downstream HO-1 and ARE-driven antioxidant enzyme upregulation.

In peritonitis, attenuation of lipid peroxidation (MDA) and preservation of antioxidant capacity (SOD) by Cur-SLNs would mitigate ROS-mediated mesothelial injury, reduce neutrophil-endothelial adhesion, and limit progression from localized peritonitis to systemic sepsis. Because NF-κB-driven

inflammation generates ROS and ROS reciprocally activate NF-κB, curcumin's ability to interrupt both arms of this positive feedback loop makes it particularly effective where inflammation and oxidative stress are tightly coupled.

### **Effects on leukocyte count, bacterial burden, and histopathology**

As summarized in Table 3, CLP-induced peritonitis resulted in significant leukocytosis (WBC 28.4±4.8 versus 9.1±1.5 ×10<sup>3</sup>/μL in sham, p<0.001), elevated peritoneal bacterial CFU count (14.8±3.2 versus 0.2±0.1 ×10<sup>4</sup>/mL, p<0.001), and severe histopathological damage (score 3.4±0.5 versus 0.5±0.3, p<0.001). Cur-SLN high dose significantly reduced WBC count (11.2±2.1 ×10<sup>3</sup>/μL, 60.6% reduction, p<0.001), peritoneal bacterial CFU (3.2±0.9 ×10<sup>4</sup>/mL, 78.4% reduction, p<0.001), and histopathological damage score (1.1±0.3; 67.6% improvement; p<0.001, d=5.59). As detailed in Table 3, the dose-dependent pattern was maintained, with Cur-SLN low dose (WBC 15.7±2.8, CFU 6.7±1.8, histopathology 1.8±0.4) and free curcumin (WBC 18.6±3.2, CFU 8.5±2.1, histopathology 2.3±0.4) showing intermediate but significant effects (all p<0.001 versus CLP-vehicle).

Table 3. Treatment effects on secondary outcomes: leukocyte count, peritoneal bacterial burden, and histopathological injury score (mean±SD, n=6 per group).

Outcome	Sham	CLP+Vehicle	CLP+Free Cur	Cur-SLN Low	Cur-SLN High
<b>WBC (10<sup>3</sup>/μL)</b>	9.1±1.5	28.4±4.8	18.6±3.2	15.7±2.8	11.2±2.1
<b>Bacterial CFU (10<sup>4</sup>/mL)</b>	0.2±0.1	14.8±3.2	8.5±2.1	6.7±1.8	3.2±0.9
<b>Histopathology score</b>	0.5±0.3	3.4±0.5	2.3±0.4	1.8±0.4	1.1±0.3

Notes: WBC, white blood cell count; CFU, colony-forming units; Cur, curcumin; SLN, solid lipid nanoparticles.

The antibacterial effect of Cur-SLNs is noteworthy, as curcumin possesses direct antibacterial activity against Gram-positive and Gram-negative organisms through membrane disruption, inhibition of FtsZ assembly, and quorum-sensing suppression.<sup>19,20</sup> Li et al.<sup>20</sup> reported that curcumin-silver nanoparticle composite films achieved 99.6% and 100% growth inhibition against *Escherichia coli* and

*Staphylococcus aureus*, respectively, while Shi et al.<sup>19</sup> and Xu et al.<sup>21</sup> confirmed potent antibacterial and anti-inflammatory effects of curcumin nanoparticle systems in vivo. Karahalioglu and Hazer<sup>22</sup> demonstrated antibacterial efficacy of curcumin-functionalized membranes against *E. coli* and *S. aureus*, and Guo et al.<sup>23</sup> reported pronounced antibacterial activity of curcumin-functionalized

surfaces. The enhanced antibacterial effect of Cur-SLNs versus free curcumin (78.4% versus 42.6% CFU reduction) likely results from nanoparticle-mediated enhancement of curcumin's interaction with bacterial membranes and prolonged release.<sup>12,13</sup>

The analysis confirmed the robustness of Cur-SLN treatment effects, with all outcome measures demonstrating large effect sizes (Cohen's *d* 4.50–

5.72) for the Cur-SLN high dose versus CLP-vehicle comparison. The ANOVA partial eta-squared values were consistently large ( $\eta_p^2$  0.89–0.96), indicating that group assignment explained 89–96% of the variance. The forest plot in Figure 3 illustrates the consistent magnitude of treatment benefit across all assessed parameters, with 95% confidence intervals lying well above the null value.

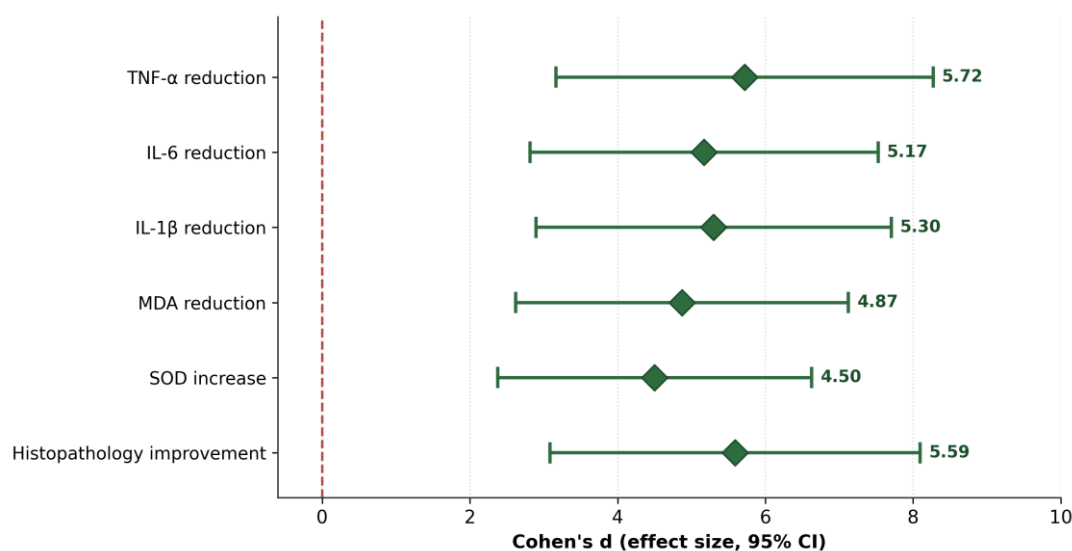


Figure 3. Forest plot of treatment effect sizes (Cohen's *d*, 95% CI) for Cur-SLN high dose versus CLP-vehicle. Diamonds represent point estimates and horizontal lines the 95% confidence intervals. All effect sizes are large and statistically significant, demonstrating robust therapeutic benefit across all measured parameters.

### Dose-response relationship and pharmacokinetic considerations

The dose-dependent pattern across the Cur-SLN low dose (50 mg/kg) and high dose (100 mg/kg) groups, detailed in Table 2 and Figure 1, provides insight into the pharmacokinetic advantages of the SLN platform. The low dose achieved approximately 47–50% cytokine reduction versus CLP-vehicle, and the high dose approximately 67–69%, indicating a near-linear dose-response relationship. Notably, the Cur-SLN low dose (50 mg/kg) produced anti-inflammatory effects comparable to or exceeding free curcumin at twice the dose (100 mg/kg), directly demonstrating the bioavailability enhancement afforded by SLN encapsulation.<sup>23,24</sup> This implies that lower therapeutic doses could achieve equivalent or superior efficacy when formulated as SLNs. The enhanced bioavailability is attributable to lipid-matrix protection from degradation, sub-200 nm

particle size (152.4±8.7 nm) enabling macrophage uptake, and a negative zeta potential (-28.6±2.1 mV) providing colloidal stability; the high entrapment efficiency (87.3±3.2%) and inter-batch reproducibility (CV <6%) confirm formulation robustness.<sup>10,11</sup>

### Clinical implications, limitations, and herbal medicine context

These findings carry implications for integrating herbal nanomedicine into peritonitis management, particularly in Southeast Asian settings where traditional medicine remains prevalent. The development of Cur-SLNs bridges traditional *Curcuma longa* knowledge with modern pharmaceutical technology, and the demonstrated anti-inflammatory, antioxidant, and antibacterial properties suggest potential as an adjunct to conventional antibiotic therapy, potentially reducing antibiotic dose requirements and mitigating antimicrobial resistance.<sup>4,9</sup> This integrative approach

aligns with the World Health Organization Traditional Medicine Strategy. Limitations warrant acknowledgment: the animal model limits direct extrapolation to humans, and the extraordinarily large effect sizes ( $d > 4.0$ ) in this controlled setting would likely translate to more moderate clinical effects; the 24-hour timepoint does not capture resolution or survival; the bacterial inoculum was not standardized; the intraperitoneal route differs from the oral route traditional for herbal medicine; and additional molecular markers (NF- $\kappa$ B p65, COX-2/iNOS, Nrf2/HO-1 protein) would strengthen mechanistic interpretation. The translational pathway should include extended survival studies, oral pharmacokinetic profiling, antibiotic-synergy assessment, stability studies under ICH Q1A conditions, and ultimately Phase I/II randomized controlled trials, positioning this study as a foundational preclinical contribution toward registration under Indonesia's BPOM fitofarmaka pathway.

#### 4. Conclusion

Curcumin-loaded solid lipid nanoparticles prepared from *Curcuma longa* L. rhizome extract significantly attenuate inflammatory cytokine cascades, reduce oxidative stress, diminish bacterial burden, and preserve peritoneal tissue integrity in a CLP-induced acute peritonitis rat model, with dose-dependent superiority over free curcumin. The Cur-SLN high dose (100 mg/kg) achieved approximately 68% reduction in pro-inflammatory cytokines (all  $p < 0.001$ ) with large effect sizes (Cohen's  $d$  4.50–5.72), attributable to enhanced NF- $\kappa$ B pathway suppression through IKK $\beta$  Cys179 modification and Nrf2-mediated antioxidant defense activation conferred by the nanoparticle delivery system. The Cur-SLN low dose (50 mg/kg) achieved anti-inflammatory effects comparable to free curcumin at double the dose, confirming the bioavailability enhancement provided by SLN technology. These findings provide compelling preclinical evidence supporting the development of Cur-SLNs as an adjunctive herbal nanomedicine for peritonitis management, representing a promising convergence

of Indonesian herbal medicine heritage and contemporary pharmaceutical innovation.

#### 5. References

1. Napolitano LM. Intra-abdominal infections. *Semin Respir Crit Care Med.* 2022; 43(1):10–27. doi:[10.1055/s-0041-1741053](https://doi.org/10.1055/s-0041-1741053)
2. Niu Y, Xu G, Zhu S, et al. NONO regulates multiple cytokine production in sepsis via the ERK1/2 signaling pathway. *Mol Immunol.* 2022; 153:94–105. doi:[10.1016/j.molimm.2022.11.017](https://doi.org/10.1016/j.molimm.2022.11.017)
3. Sarawi WS, Alhusaini AM, Fadda LM, et al. Nano-curcumin prevents cardiac injury, oxidative stress and inflammation, and modulates TLR4/NF- $\kappa$ B and MAPK signaling in copper sulfate-intoxicated rats. *Antioxidants (Basel).* 2021; 10(9):1414. doi:[10.3390/antiox10091414](https://doi.org/10.3390/antiox10091414)
4. Lepe JA, Martínez-Martínez L. Resistance mechanisms in Gram-negative bacteria. *Med Intensiva (Engl Ed).* 2022; 46(7):392–402. doi:[10.1016/j.medine.2022.05.004](https://doi.org/10.1016/j.medine.2022.05.004)
5. Saleem U, Chauhdary Z, Bakhtawar Z, et al. Curcuminoids-enriched extract and its cyclodextrin inclusion complexes ameliorates arthritis in complete Freund's adjuvant-induced arthritic mice via modulation of inflammatory biomarkers and suppression of oxidative stress markers. *Inflammopharmacology.* 2023; 31(6):3047–3062. doi:[10.1007/s10787-023-01370-2](https://doi.org/10.1007/s10787-023-01370-2)
6. Murugan S, Solanki H, Purusothaman D, et al. Safety evaluation of standardized extract of *Curcuma longa* (NR-INF-02): a 90-day subchronic oral toxicity study in rats. *Biomed Res Int.* 2021; 2021:6671853. doi:[10.1155/2021/6671853](https://doi.org/10.1155/2021/6671853)
7. Zhai F, Wang J, Wan X, et al. Dual anti-inflammatory effects of curcumin and berberine on acetaminophen-induced liver injury in mice by inhibiting NF- $\kappa$ B activation via PI3K/AKT and PPAR $\gamma$  signaling pathways. *Biochem Biophys Res Commun.* 2024; 734:150772. doi:[10.1016/j.bbrc.2024.150772](https://doi.org/10.1016/j.bbrc.2024.150772)

8. Tanase DM, Gosav EM, Anton MI, et al. Oxidative stress and NRF2/KEAP1/ARE pathway in diabetic kidney disease (DKD): new perspectives. *Biomolecules*. 2022; 12(9):1227. doi:[10.3390/biom12091227](https://doi.org/10.3390/biom12091227)
9. Montanino C, Farinella F, De Felice B, et al. The potential systemic anti-inflammatory effect of turmeric dried extract. *Endocr Metab Immune Disord Drug Targets*. 2025; 25(14):1191–1198. doi:[10.2174/0118715303329562241116045410](https://doi.org/10.2174/0118715303329562241116045410)
10. Khatri B, Thakkar V, Dalwadi S, et al. Preparation and characterization of solid lipid nanoparticles containing artemisinin and curcumin. *Pharm Nanotechnol*. 2025; 13(1):199–211. doi:[10.2174/0122117385296893240626061552](https://doi.org/10.2174/0122117385296893240626061552)
11. Gonçalves RFS, Fernandes JM, Martins JT, et al. Incorporation of curcumin-loaded solid lipid nanoparticles into yogurt: tribo-rheological properties and dynamic in vitro digestion. *Food Res Int*. 2024; 181:114112. doi:[10.1016/j.foodres.2024.114112](https://doi.org/10.1016/j.foodres.2024.114112)
12. Hamdalla HM, Ahmed RR, Galaly SR, et al. Ameliorative effect of curcumin nanoparticles against monosodium iodoacetate-induced knee osteoarthritis in rats. *Mediators Inflamm*. 2022; 2022:8353472. doi:[10.1155/2022/8353472](https://doi.org/10.1155/2022/8353472)
13. Chae J, Choi Y, Hong J, et al. Anticancer and antibacterial properties of curcumin-loaded mannosylated solid lipid nanoparticles for the treatment of lung diseases. *ACS Appl Bio Mater*. 2024; 7(4):2175–2185. doi:[10.1021/acsabm.3c01145](https://doi.org/10.1021/acsabm.3c01145)
14. Javed C, Noreen R, Niazi SG, et al. Anti-gouty arthritis and anti-inflammatory effects of curcumin nanoparticles in monosodium urate crystals induced Balb/C mice. *Inflammopharmacology*. 2024; 32(3):1929–1940. doi:[10.1007/s10787-024-01450-x](https://doi.org/10.1007/s10787-024-01450-x)
15. Chen T, Zhuang B, Huang Y, et al. Inhaled curcumin mesoporous polydopamine nanoparticles against radiation pneumonitis. *Acta Pharm Sin B*. 2022; 12(5):2522–2532. doi:[10.1016/j.apsb.2021.10.027](https://doi.org/10.1016/j.apsb.2021.10.027)
16. Zou J, Guo J, Hu G, et al. Curcumin attenuates PD-L1-positive neutrophil-induced T-lymphocyte apoptosis and alleviates lung injury during sepsis in rats. *Discov Med*. 2025; 37(195):772–782. doi:[10.24976/Discov.Med.202537195.67](https://doi.org/10.24976/Discov.Med.202537195.67)
17. Wang L, Wu N, Zhang W, et al. Curcumin alleviates sepsis-associated acute kidney injury potentially by inhibiting ferroptosis through the ACSL4/GPX4 signaling pathway. *Drug Dev Res*. 2025; 86(7):e70181. doi:[10.1002/ddr.70181](https://doi.org/10.1002/ddr.70181)
18. Wang S, Zhao P, Zhang Y, et al. The therapeutic effects of curcumin in early septic acute kidney injury: an experimental study. *Drug Des Devel Ther*. 2021; 15:4243–4255. doi:[10.2147/DDDT.S332623](https://doi.org/10.2147/DDDT.S332623)
19. Shi C, Zhang Y, Wu G, et al. Hyaluronic acid-based reactive oxygen species-responsive multifunctional injectable hydrogel platform accelerating diabetic wound healing. *Adv Healthc Mater*. 2024; 13(4):e2302626. doi:[10.1002/adhm.202302626](https://doi.org/10.1002/adhm.202302626)
20. Li S, Wei N, Wei J, et al. Curcumin and silver nanoparticles loaded antibacterial multifunctional pectin/gelatin films for food packaging applications. *Int J Biol Macromol*. 2024; 266(Pt 1):131248. doi:[10.1016/j.ijbiomac.2024.131248](https://doi.org/10.1016/j.ijbiomac.2024.131248)
21. Xu S, Hu B, Dong T, et al. Alleviate periodontitis and its comorbidity hypertension using a nanoparticle-embedded functional hydrogel system. *Adv Healthc Mater*. 2023; 12(20):e2203337. doi:[10.1002/adhm.202203337](https://doi.org/10.1002/adhm.202203337)
22. Karahalioglu Z, Hazer B. Curcumin- and quercetin-functionalized polypropylene membranes as active food packaging material. *J Food Sci*. 2024; 89(10):6575–6589. doi:[10.1111/1750-3841.17333](https://doi.org/10.1111/1750-3841.17333)
23. Guo Q, Li P, Zhang Y, et al. Polydopamine-curcumin coating of titanium for remarkable antibacterial activity via synergistic

photodynamic and photothermal properties.  
Photochem Photobiol. 2024; 100(3):699–711.  
doi:[10.1111/php.13870](https://doi.org/10.1111/php.13870)

24. Rostamzadeh F, Jafarnejad-Farsangi S, Ansari-Asl Z, et al. Treatment for myocardial infarction: in vivo evaluation of curcumin-loaded PEGylated-GQD nanoparticles. J Cardiovasc Pharmacol. 2023; 81(5):361–372.  
doi:[10.1097/FJC.0000000000001410](https://doi.org/10.1097/FJC.0000000000001410)